Earth Planet. Sci. Lett. 671 (2025) 119686

Contents lists available at ScienceDirect

Earth and Planetary Science Letters

journal homepage: www.elsevier.com/locate/epsl

Structural controls on simultaneous earthquake clustering and normal fault synchronization

F. Iezzi [a,*], C. Sgambato [b], G. Roberts [b], Z. Mildon [c], J. Robertson [b], J. Faure Walker [d], I. Papanikolaou [e], A.M. Michetti [f,g], S. Mitchell [b], R. Shanks [h], R. Phillips [i], K.J.W. McCaffrey [j], E. Vittori [k]

[a] Department of Earth Sciences, Environment and Resources, University of Naples Federico II, Naples, Italy
[b] Department of Natural Sciences, Birkbeck College, University of London, UK
[c] School of Geography, Earth and Environmental Sciences, University of Plymouth, UK
[d] Department of Risk and Disaster Reduction, University College of London, UK
[e] Department of Natural Resources Development and Agricultural Engineering, Laboratory of Mineralogy and Geology, Agricultural University of Athens, Athens, Greece
[f] Dipartimento di Scienza e Alta Tecnologia, Università degli Studi dell'Insubria, Como, Italy
[g] Istituto Nazionale di Geofisica e Vulcanologia, Sezione di Napoli Osservatorio Vesuviano, Naples, Italy
[h] Scottish Universities Environmental Research Centre, Glasgow, UK
[i] School of Earth and Environment, University of Leeds, Leeds, UK
[j] Department of Earth Sciences, Durham University, Durham, UK
[k] IGG-CNR Florence, Italy

ARTICLE INFO

Editor: J.P. Avouac

Keywords:
Earthquake geology
Earthquake clusters
^{36}Cl cosmogenic dating
Stress transfer
Viscous flow
seismic hazard

ABSTRACT

Slip-rate fluctuations over multiple seismic cycles are a key factor to consider regarding the behaviour of active faults, as they are associated with clustering of earthquakes in space and time and may alter the earthquake recurrence on neighbouring faults. However, processes that produce slip-rate fluctuations are yet to be fully defined. This paper tests whether the interaction between neighbouring along-strike brittle faults/viscous shear-zones can produce slip-rate fluctuations associated with simultaneous earthquake clustering and fault synchronization. To achieve this, we study nine normal faults/shear zones of the Central Apennines fault system (Italy), organised in six different arrangements of along-strike pairs with different values of fault spacing and strike variation. We combine cosmogenic ^{36}Cl dating of tectonically exhumed fault planes and modelling of the mutual differential stress changes within the fault/shear-zone pairs. Our results reveal a mechanism for the occurrence of simultaneous earthquake clusters, based on the synchronization of high driving stresses for the viscous shear-zones underneath the brittle faults, that is strongly controlled by the spacing and strike changes between faults/shear-zone pairs. In settings with low along-strike spacing and minimal strike change between neighbouring faults/shear-zones, earthquake clusters cause positive differential stress variations on neighbouring shear-zones of sufficient magnitude to induce positive slip-rate variations on their overlying brittle faults. This in turn produces positive feedback that sustains the occurrence of earthquake clusters that will continue to positively load the neighbouring shear zones. This positive feedback mechanism contributes to the understanding of fault dynamics at multiple timescales and to seismic hazard assessments.

1. Introduction

Slip-rate fluctuations characterize the behaviour of active faults, being associated with the clustering of earthquakes in space and time within fault systems (e.g. Cowie et al., 2017). Understanding the processes that control such behaviour is crucial for seismic hazard

* Corresponding author.
E-mail addresses: francesco.iezzi@unina.it (F. Iezzi), c.sgambato@bbk.ac.uk (C. Sgambato), g.roberts@bbk.ac.uk (G. Roberts), zoe.mildon@plymouth.ac.uk (Z. Mildon), j.robertson@bbk.ac.uk (J. Robertson), j.faure-walker@ucl.ac.uk (J. Faure Walker), i.pap@aua.gr (I. Papanikolaou), alessandro.michetti@uninsubria.it (A.M. Michetti), sam.mitchell@bbk.ac.uk (S. Mitchell), richard.shanks@glasgow.ac.uk (R. Shanks), tighnadarroch@gmail.com (R. Phillips), k.j.w.mccaffrey@durham.ac.uk (K.J.W. McCaffrey), tizianovittori@gmail.com (E. Vittori).

https://doi.org/10.1016/j.epsl.2025.119686
Received 24 June 2025; Accepted 9 October 2025
Available online 22 October 2025

assessments, as slip-rate fluctuations will impose a variability in the earthquake recurrence rates that alters key parameters for seismic hazard estimations, such as the earthquake recurrence interval (Tmean) and its Coefficient of Variation (CV) (Cowie et al., 2012; Pace et al., 2014; Visini and Pace, 2014). Processes causing slip-rate fluctuations are debated and observations have rarely been reproduced through modelling, hence it is difficult to envisage mechanisms of fault synchronization and, more in general, to include slip-rate fluctuations into seismic hazard assessments. Strain release on brittle faults is largely controlled by viscous flow along shear-zones located on the downward propagation of faults underneath the brtittle/ductile transition (Ellis and Stockhert, 2004; Dolan et al., 2007; Oskin et al., 2008; Cowie et al., 2013; Fossen and Cavalcante, 2017). This is supported by the notion that variations in the differential stress on the shear-zones coincide with variations in the strain-rates due to the power law relationship for dislocation creep that links strain-rate ε and differential stress σ by a coefficient $n = \sim 3$: $\varepsilon \propto \sigma^n$ (Eq. 1; Hirth et al., 2001; Cowie et al., 2013). This power law relationship resembles the one that Cowie et al. (2013) identifies linking strain-rates derived from slip-rate measurements on fault scarps averaged over 15±3 ka and the topographic elevation h: $\varepsilon \propto h^n$, where $n = 3$. The consistency between the two power laws suggests that slip-rates on the brittle faults are driven by the strain-rate associated with the underlying viscous shear-zones, implying consistency between the finite strain within the brittle and viscous crust over multiple seismic cycles. This also implies that strain-rates averaged over time periods containing multiple earthquake cycles, a time period longer than that for postseismic deformation from a single earthquake, are the same in the upper and middle crust (Shimamoto and Noda, 2014; Allison and Dunham, 2018). Dolan and Meade (2017) suggested that slip-rate fluctuations on brittle faults may be controlled by processes of strain hardening and annealing associated with viscous slip on shear-zones in the lower crust. Specifically, high viscous strain-rates increase the slip-rate of the brittle fault, but also lead to strain-hardening, that in turn work to halt the occurrence of the earthquake cluster on the brittle fault above. Slip is then transferred onto neighbouring shear-zones that experienced low strain-rates and hence had time to anneal. This process suggests therefore that slip-rate fluctuations are controlled by processes on a longer time scale than those of stress changes associated with single earthquakes. Mildon et al. (2022) and Roberts et al. (2024) suggested that slip-rate fluctuations associated with earthquake clustering encompassing multiple seismic cycles may be a result of differential stress changes between brittle faults and their underlying viscous shear-zones (Fig. 1a). In these studies, the authors show that it is possible to replicate measured out-of-phase clustering patterns on brittle faults by calculating differential stress variations on their viscous shear-zones due to stress transfer from the brittle faults and vice versa, and between neighbouring fault/shear-zone structures. Mildon et al. (2022) and Roberts et al. (2024; 2025) show that earthquake clusters can produce negative changes of differential stress on across-strike brittle faults/viscous shear-zones of magnitude large enough to decrease their activity and lead them into longer periods of no/little fault activity (anticlusters). However, less is known about the effect of

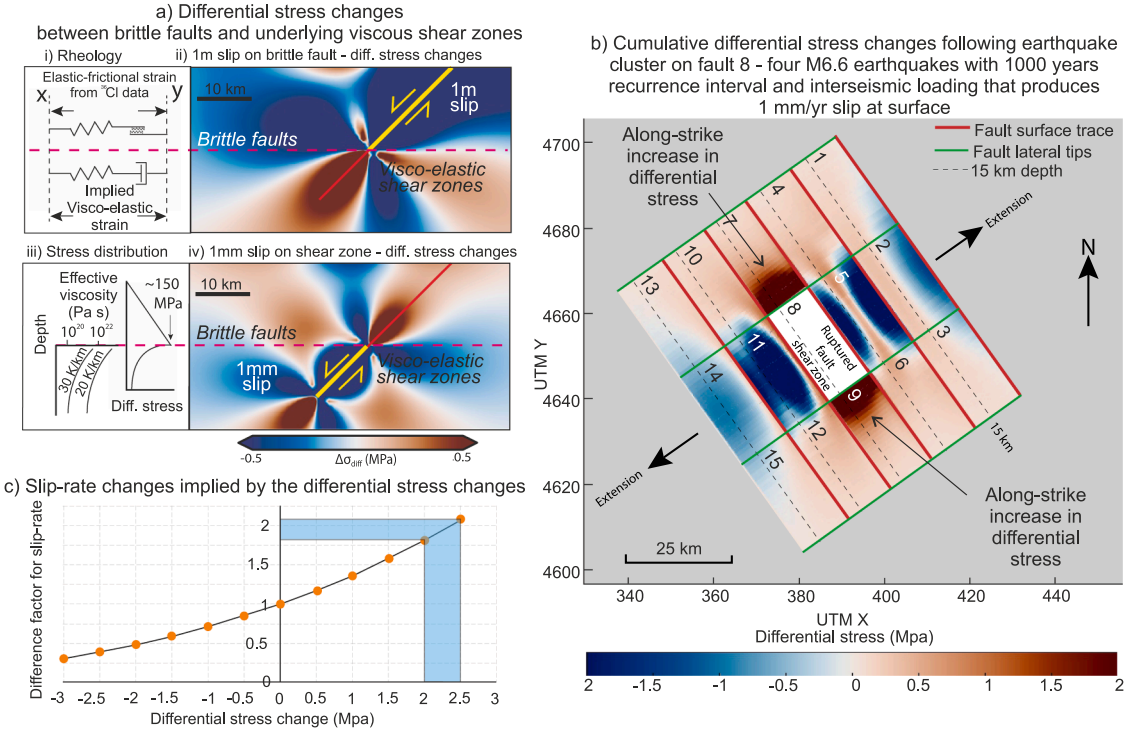

Fig. 1. Background knowledge on differential stress changes between brittle faults and viscous shear-zones. a) Differential stress changes between brittle faults and visco-elastic shear-zones. i) shows that elastic brittle strain in the upper crust is matched by visco-elastic strain at depth over multiple earthquake cycles; ii) differential stress changes associated with 1 m coseismic slip on the brittle fault: the underlying shear-zone is positively loaded by the fault slip; iii) background differential stress and viscosity profiles over depth; iv) differential stress changes associated with 1 mm slip on the visco-elastic shear-zone, which occurs every year is the fault slip-rate is 1 mm/yr: the overlying fault receive a positive differential stress change. Panels ii) and iv) show that slip on either brittle fault or visco-elastic shear-zone causes positive differential stress changes on the other element, prompting a positive feedback mechanism for the onset of earthquake clusters. b) Differential stress changes associated with the occurrence of an earthquake cluster on fault 8. The earthquake cluster is characterized by four M6.6 earthquake, recurrence interval of 1000 years and 1 mm per year of interseismic slip in the shear-zone. This panel shows that along-strike faults receive a positive differential stress variation. c) Slip-rate changes implied by differential stress changes. This plot shows that positive differential stress changes are linked to a positive difference factor for slip-rate. The pale blue box shows that differential stress changes of 2–2.5 MPa, values that can be achieved during clusters (see Fig. 1b), coincides with difference factors for slip-rates of about 2, i.e. they can double the slip-rate of the brittle fault. These figures are modified from Roberts et al. (2024) and references therein.

stress interactions between along-strike brittle faults/shear-zones over timescales that encompasses multiple seismic cycles. This paper explores the hypothesis that positive differential stress changes between along-strike faults/shear-zones may be responsible for the occurrence of simultaneous earthquake clustering and fault synchronization.

The background of this hypothesis is based on physical mechanisms that suggest stress transfer between neighbouring faults as the triggering mechanism for earthquake clusters. For instance, Coulomb stress changes and postseismic viscoelastic relaxation processes were proposed as explanations for the occurrence of decadal earthquake clusters (e.g. Mildon et al., 2017; Verdecchia et al., 2018). Longer earthquake clusters, lasting hundreds to thousands of years (e.g. Sieh et al., 2008; Goldfinger et al., 2013; Salditch et al., 2020 and references therein), have been associated with positive stress coupling between neighbouring along-strike faults (the "phase locking" mechanism, Scholz (2010)). The phase locking mechanism implies that, when two faults are positively coupled during the growth/propagation/linkage history of the fault system, each earthquake will produce stress changes that advance the seismic cycle of the receiver fault until the two seismic cycles become synchronized and their earthquake clusters become simultaneous. However, this mechanism does not include the role that differential stress changes play on the strain-rate of neighbouring viscous shear-zones and how this influences the occurrence of earthquake clusters. For instance, Roberts et al. (2024) show that an earthquake cluster, formed by (i) four M6.6 1 m surface slip events and (ii) three intervening periods of interseismic loading each lasting 1000 years during which the fault is loaded by viscous flow on the underlying shear-zone, produces positive differential stress changes that can be larger than 2 MPa on neighbouring along-strike fault/shear-zones (Fig. 1b). To evaluate the impact of such differential stress changes on the fault slip-rates, Roberts et al. (2024) calculated the difference factor of the slip-rate during earthquake clusters by dividing the slip-rate implied from the strain-rates following the differential stress changes with the fault long-term slip-rate. The authors show that 2–2.5 MPa coincides with slip-rate difference factors of the order of 2, i.e. the slip-rate of a brittle fault can double due to positive differential stress changes associated with a neighbouring cluster (Fig. 1c). Hence, it seems plausible that differential stress changes between positively coupled along-strike fault/shear-zones may induce slip-rate increases associated with earthquake clusters that last several millennia, and this may explain the phenomenon of fault synchronisation.

To test this hypothesis, we use data obtained from cosmogenic ^{36}Cl dating of neighbouring fault planes to constrain whether particular faults have clusters occurring over the same time interval (i.e. synchronous) or not, and whether the geometries of faults favour synchronisation or not. This is because multiple papers have shown the reliability of modelling ^{36}Cl fault scarp concentrations, in some cases with Bayesian approaches, to derive continuous records of slip-rate covering up to several tens of millennia, unveiling periods of rapid slip and phases of little/no fault activity (Palumbo et al., 2004; Schlagenauf et al., 2010; Benedetti et al., 2013; Tesson et al., 2016; Cowie et al., 2017; Beck et al., 2018; Mozafari et al., 2019; Tesson and Benedetti, 2019; Goodall et al., 2021; Iezzi et al., 2021; Mildon et al., 2022; Dawood et al., 2024; Roberts et al., 2024; 2025). These studies have identified periods of time lasting just a few millennia or less that are (a) marked by slip that is several times larger than the slip expected for a single earthquake given fault length to coseismic slip scaling information (e.g. Wells and Coppersmith 1994), and (b) close to or shorter in duration than average recurrence intervals for surface faulting earthquakes in the given region. The implied slip-rate in these time periods exceed that measured over the entire Holocene or since the Last Glacial Maximum (LGM). The time periods with anomalously high slip-rate that cannot be explained by a single surface faulting earthquake have been interpreted as temporal clusters of surface faulting earthquakes (e.g. Roberts et al., 2025). We compute the differential stress changes associated with such temporal earthquake clusters on along-strike brittle faults/viscous shear-zones. This allows us to explore the simultaneous activity of faults over timescales that encompasses single events, verifying whether (1) neighbouring along-strike faults experience simultaneous earthquake clustering, and (2) whether these clusters produce differential stress changes of sufficient magnitude to lead faults towards synchronization.

This study focuses on six different arrangements of along-strike adjacent normal fault (hereinafter defined fault pairs) located in the Central Apennines (Italy), each characterized by variable spacing and strike values between the two faults (Fig. 2). We examine whether earthquake clusters occur over the Late Pleistocene-Holocene and the degree of synchronicity between neighbouring along-strike faults. For every fault/shear-zone pair, we compute the differential stress changes associated with earthquake clustering on each fault/shear-zone. We identify specific fault settings and geometries that favour/penalise simultaneity of earthquake clusters and hence fault synchronization. We discuss the results of our work in terms of faulting dynamics and seismic hazard assessments.

2. Geological background

The Central Appennines are a Mio-Pliocene NE-SW verging fold-and-thrust belt that thrusted Meso-Cenozoic limestones onto Miocene flysch deposits, in response to the collision of European and African tectonic plates (Anderson and Jackson, 1987). Since 2–3 Ma, the region has experienced a SW-NE oriented extensional regime that caused the onset of normal faulting, which dissected the existing thrust belt and generated intermontane basins (Cavinato and Celles, 1999). Normal faults are generally 20–40 km long, have NW-SE strike and overall dip-slip kinematics, and form a dense array showing both across- and along-strike arrangements (Boncio et al., 2004; Roberts and Michetti, 2004; Pizzi and Galadini, 2009). These faults have the potential to release medium-to-large magnitude earthquakes (6.5–7.0), as shown by instrumental and historical seismicity (CPTI15; Rovida et al., 2020; 2022) and paleoseismological investigations (e.g. Galli et al., 2008; Cinti et al., 2021). The regional horizontal extension is up to 3 mm/yr, a value in agreement with fault slip data (Faure Walker et al., 2010; 2012), geodetic measurements (D'Agostino et al., 2011; Devoti et al., 2017) and InSAR analysis (Daout et al., 2023).

The faults studied herein are the Pescasseroli fault, the Fucino fault, the Scanno fault, Roccapreturo fault, the Paganica-San Demetrio (PSD) fault, the Mt. Marine fault, the Barisciano-Mt. Stabiata fault, the Campo Imperatore fault and the Laga fault (Fig. 2). Their Late Pleistocene-Holocene activity has been shown by combinations of recent surface-rupturing earthquakes, paleoseismological investigations and offset of post-Last Glacial Maximum (LGM) landforms (e.g. Pantosti et al., 1996; Galadini and Galli, 1999, 2003; Roberts and Michetti, 2004; Papanikolaou et al., 2005; Boncio et al., 2010; Faure Walker et al., 2010; Galli et al., 2011; Falcucci et al., 2015; Blumetti et al., 2017; Mildon et al., 2019; Faure Walker et al., 2019, 2021; Cinti et al., 2021; Galli et al., 2022; Iezzi et al., 2023). Cosmogenic ^{36}Cl dating of tectonically exhumed fault planes show a clustered behaviour of Central Apennine faults during the Late Pleistocene-Holocene (Benedetti et al., 2013; Cowie et al., 2017; Goodall et al., 2021; Mildon et al., 2022; Roberts et al., 2024; 2025). Overall, the available literature shows that faults in this region (i) are active during the Late Pleistocene-Holocene; (ii) can release surface-rupturing earthquakes, meaning that fault scarps grow by repeating earthquakes through time; (iii) their fault scarps started growing since the demise of the LGM, when warmer climate conditions allowed for the preservation of growing fault scarps, that were progressively eroded in glacial conditions (e.g. Piccardi et al., 1999); (iv) their activity is clustered, with periods of rapid and no/slow slip alternating through time during the slip history of a fault; (v) earthquake clustering can be explained by fluctuations of differential stress associated with the interaction of brittle faults/viscous shear-zones, but such fluctuations have not been modelled for the fault pairs we study.

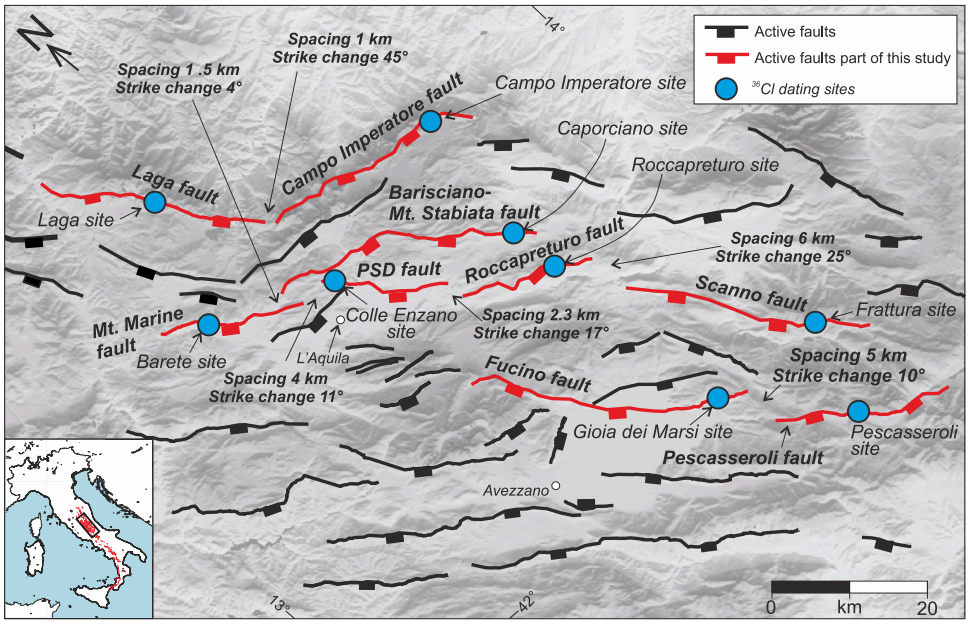

Fig. 2. Map of the studied faults. In red are active faults studied herein. In black are other main active faults. Fault traces are modified after the Fault2SHA database (Faure Walker et al., 2021). Blue markers are locations of cosmogenic ^{36}Cl dating sites performed within this study. Site names are referred to the NERC repository within the National Geoscience Data Centre (NGDC) of the British Geological Society (https://www.bgs.ac.uk/services/ngdc/accessions/index.html#item128345) and Roberts et al. (2025). PSD fault: Paganica-San Demetrio fault. Information on fault spacing, measured as tip-to-tip distance, and strike changes between each fault pair are shown in the map.

3. Approach and methods

The workflow is characterized by three main steps: 1- identification of suitable fault pairs, 2- modelling of fault slip histories through cosmogenic ^{36}Cl dating of fault planes, 3- computation of the differential stress variations within each fault pair. The ^{36}Cl data were collected during field campaigns between 2008 and 2015, with data published in Roberts et al. (2025).

3.1. Identification of fault pairs

We identified sets of adjacent along-strike faults with ^{36}Cl cosmogenic results available in Roberts et al. (2025). The selected fault pairs have (i) different values of fault spacing and end-on/overlapping arrangements, and (ii) variable strike changes between the two faults of the pair. The fault spacing is measured as the end-to-end distance between the adjacent segments. In case two fault segments overlap, spacing is measured as the minimum distance between the two segments. The average strike is measured from end-to-end, to avoid potential bias due to minor scale structural complexities and segmentation. The variability in the structural relationships between the two faults is important because it allows us to explore whether specific along-strike arrangements may favour simultaneous earthquake clustering and therefore fault synchronicity.

3.2. Cosmogenic ^{36}Cl dating of fault planes

We performed modelling of the cosmogenic ^{36}Cl data for the nine faults to retrieve slip-rate fluctuations over a time that encompasses multiple seismic cycles, i.e. since the demise of the LGM. The sampling occurred on fault planes located within scarps offsetting periglacial slopes, which stabilised during the last glaciation and preserved since then (e.g. Bosi, 1975; Piccardi et al. 1999; Roberts and Michetti, 2004; Cowie et al., 2017). The sampling sites were chosen to constrain exhumation due only to tectonic movement, excluding sites affected by erosional/depositional processes (See Electronic Supplement ES1). To do so, sampled fault scarps needed to show specific characteristics, following Cowie et al. (2017): (i) fault scarps are undisturbed by post-glacial erosion and sedimentation on the upper and lower slopes and have planar free faces; (ii) hanging-wall and footwall cut-offs are sub-horizontal and sub-parallel, suggesting that these have not been altered through time since the scarp started growing; (iii) millimetre scale striations are present onto fault planes, testifying very low erosion of the slickenside since its exhumation. Post-LGM throws were measured by building along-strike topographic profiles across the fault scarps using a 1 m solid ruler and LiDAR surveys, where possible (see Electronic Supplement ES1). As ^{36}Cl is accumulated within the first 1–2 m below the surface (e.g. Schlagenauf et al., 2010), 1 m deep trenches were excavated in front of the sampled fault planes to collect sub-surface samples. This allows for better constraining of the sub-surface ^{36}Cl production rate and of the most recent slip history of the fault. Density of the hanging-wall colluvial material was measured for some sites by weighing the extracted material of each layer recognised in the trench stratigraphy and measuring the dimensions of the layer itself.

Samples for ^{36}Cl measurements were collected up the fault plane, following the trend and plunge of the slip vector as indicated by striations. Fault samples were $2 \times 5 \times 20$ cm in size and close to 2.7 g/cm^3 in density. Fault samples were collected both with semi-continuous and discontinuous sample ladders. In the latter arrangement, the spacing between samples is up to 20–30 cm, with an average of about 3.5

samples per metre. The different sampling approaches do not alter our results, because it has been shown that it is possible to obtain similar results (i.e. similar slip histories) by degrading continuous sampling down to a quarter of the samples, with sample spacing as low as 1 sample per metre (see Supplementary Material S3c of Iezzi et al. (2021) and Supplementary Fig. 14 from Mildon et al. (2022)). Hence, both the semi-continuous and discontinuous sampling approaches provide robust and reliable slip histories.

Samples were prepared following the approach of Stone et al. (1996) and Cowie et al. (2017). Rock crushing and clean-room chemistry were performed at University of Leeds, and the AMS analysis to determine ^{36}Cl concentrations was performed at SUERC laboratory in East Kilbride.

Fault slip histories are modelled using the Beck et al. (2018) code (Fig. 3). This code uses a Monte Carlo Markov Chain reversible jump approach that iterates the slip history several million times and forward models expected ^{36}Cl concentrations until it minimizes the misfit between the measured and modelled ^{36}Cl concentrations. This is achieved by using parallel Markov chains, whose convergence towards stable results is progressively quantified and eventually confirmed by a Gelman-Rubin test. The code requires knowledge on the chemical composition of the rock samples and of the hanging wall colluvial material from each site, elevation above sea level and latitude of the sampling sites, the fault offset, dip values of the upper slope, fault plane and lower slope (see Electronic Supplement ES2). The Beck et al. (2018) code iterates colluvial densities, production parameters such as the rates of production and attenuation lengths associated with spallogenic and muonic production, as well as both the number of slip events and displacement sizes rather pre-defining them, and is best interpreted in terms of slip-rates pulses and fluctuations, rather than single slip events. The code iterates the aperiodicity parameter and the mean recurrence interval to find solutions that best fit the data, without forcing solutions that fits pre-fixed arbitrary parameters (Electronic Supplement ES3). We set the code to choose slip histories through a Brownian-passage-time model of earthquake recurrence interval back to 120 ka, with preservation of scarps through surface faulting and low erosion allowed from as far back as 80 ka. This is because previous papers have suggested that, in places, fault scarps may be older than the expected age of ~15 ± 3 ka (Mechernich et al., 2018; 2023; Iezzi et al., 2021), a time when the demise of the high erosion rates during LGM is expected to allow stabilisation and preservation of surface-faulting scarps (e.g. Piccardi et al., 1999; Roberts and Michetti 2004). The presence of older fault scarps may suggest that locally erosional processes associated with glacial conditions were not strong enough to completely erase growing fault scarps; it also allows modelled sub-surface production to be influenced by possible fluctuating slip-rate prior to scarp preservation rather than a single imposed scenario for slip and ^{36}Cl production.

Several other codes for modelling ^{36}Cl concentrations are available (Schlagenhauf et al., 2010; Cowie et al., 2017; Beck et al., 2018; Tikhomirov et al., 2019; Tesson and Benedetti, 2019). We used the Beck et al. (2018) code because (1) it deals with early ^{36}Cl concentrations by allowing the iteration of slip-rates prior to the demise of the LGM, (2) it iterates the slip per each event; (3) it iterates ^{36}Cl production parameters described above; (4) it tests for the convergence of the parallel Markov Chains through the Gelman-Rubin test.

The retrieved slip histories are plotted in the form of the least squares solution of the modelling and the ensemble of the best 10,000 least squares solutions (although least squares values are calculated for all solutions numbering many hundreds of thousands to millions of solutions), plus the full posterior distribution of highest likelihood solutions (displayed as the median and 90 % confidence values through time from all solutions after 50 % burn-in with bins every 500 years). Results of the Beck et al. (2018) code are representative of changes in slip-rate and should not be interpreted to identify timings and amount of single slip events. We interpret these results for identifying earthquake clusters, during which faults cumulated a large amount of slip in a short period of time. Specifically, earthquake clusters were identified as short periods of time during which the accumulated slip is larger than the maximum displacement (Dmax) expected by the Dmax/fault length scaling relationship of Wells and Coppersmith (1994), i.e. the amount of slip could not be produced by single but rather multiple earthquakes, occurring over a time period that indicates a slip-rate higher than that defined by the slip-rate averaged over the entire recovered slip history. The duration of each cluster is established by identifying time windows during which the modelling records rapid increases for slip-rate in both the least squares solution and the ensemble of the top 10,000 least squares solutions, and these are typically supported by the median and 90 % confidence limits for the posterior distribution after 50 % burn-in. We consider the modelled slip histories as representative of the overall fault behaviour as they represent slip-rate variations built over multiple seismic cycles, hence they overcome the effects of floating partial rupture events. This is supported by findings of Goodall et al. (2021), which shows that ^{36}Cl dating performed on multiple sites along a fault provide slip histories with the same long-term preservation age and similar patterns of slip-rate variability.

We define two clusters as simultaneous when they occur during coincident time intervals on adjacent faults, i.e. the two faults record rapid slip increases during the same time interval. Specifically, we interpret simultaneous earthquake clusters in situations where (i) clusters overlap for their entire duration or where (ii) shorter clusters occur during longer clusters on a neighbouring fault. We define non-synchronous clusters when, meanwhile one fault records a large slip-rate increase, the adjacent fault records no/low values of slip-rate during the same time window.

3.3. *Differential stress modelling – reasoning and approach*

The state of stress of active faults is strongly influenced by complex interactions between brittle faults and their underlying shear-zones, and between neighbouring paired faults/shear-zones. Earthquake slip produces variations in static Coulomb and differential stresses onto neighbouring faults and their underlying shear-zones (e.g. King et al., 1994; Ellis and Stockhert, 2004). Variations in differential stress for shear-zones produce variations of their strain-rates, as these two dimensions are linked by the flow law for dislocation creep, for example for quartz, by:

$$\varepsilon = AfH_2O^m(\sigma_1 - \sigma_3)^n \exp\left(-\frac{Q}{RT}\right) \quad (2)$$

where ε is the strain-rate, A is a material parameter, fH_2O is the water fugacity, m is the water fugacity exponent, $\sigma_1 - \sigma_3$ is the differential

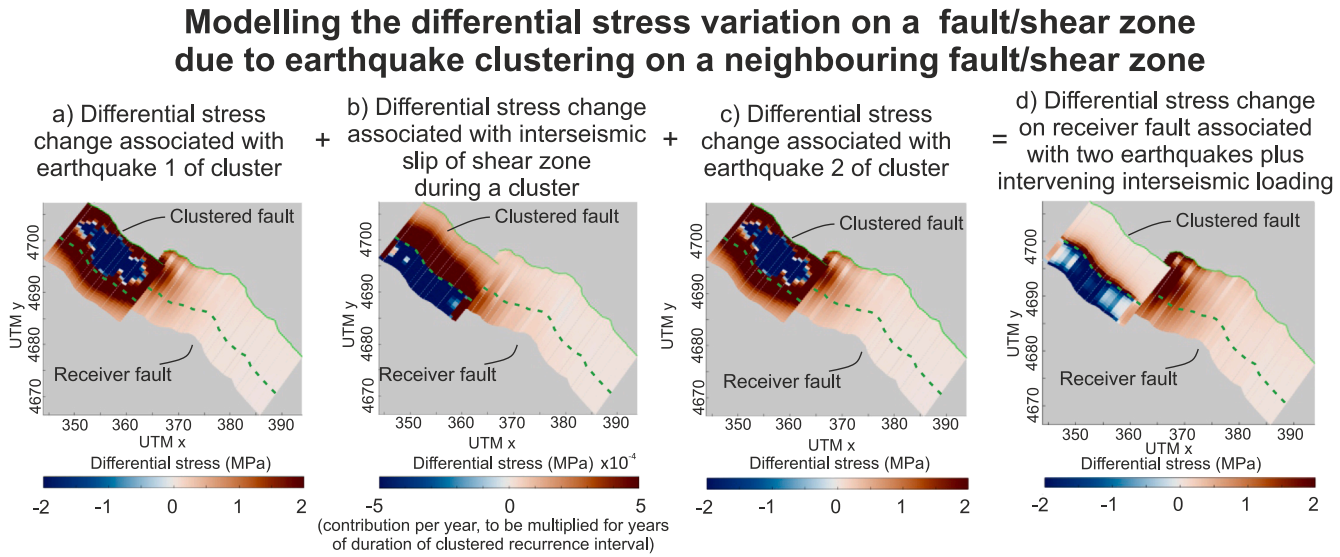

Fig. 3. Modelling approach for deriving the differential stress change imparted on to a receiver fault due to earthquake clustering occurring on a neighbouring fault/shear-zone. Solid green line is the fault surface trace. Dashed green line is the limit between brittle fault and viscous shear-zone. Each plot is obtained with Coulomb 3.4 (Toda et al., 2005).

stress, n is the differential stress exponent, Q is the activation energy, R is the ideal gas constant and T is the absolute temperature (Hirth et al., 2001). Although some of the stress changes on shear-zones may be dissipated by postseismic relaxation (Ellis and Stockhert, 2004; Verdecchia et al., 2018), the finite strain accommodated by the brittle fault must equal the finite strain accommodated by the viscous strain on shear-zones over multiple seismic cycles due to the necessity of strain compatibility with depth, implying consistency between slip-rates of the brittle faults and strain-rates of the viscous shear-zones (e.g. Cowie et al., 2013; Shimamoto and Noda, 2014). Mildon et al. (2022) and Roberts et al. (2024) suggest that differential stress changes on shear-zones produce changes in their strain-rate that in turn will drive changes in the strain-rate on the overlying brittle faults, producing slip-rate variability and temporal earthquake clustering. They have shown that the magnitudes of the implied differential stress changes and related strain-rate changes are sufficient to produce slip-rate variations on overlying brittle faults observed over multiple seismic cycles using cosmogenic ^{36}Cl measurements from central Italy, but not on the fault pairs we study. Following this, and to comply with the aim of this paper, we set up the following approach to test whether positive differential stress variations can accelerate the seismic cycles of faults up to a point that the differential stress increases can explain the occurrence of simultaneous along-strike earthquake clustering and hence be a plausible explanation for fault synchronization.

To model differential stress changes associated with clusters, we replicate the clusters derived with ^{36}Cl dating within Coulomb 3.4 (Toda et al., 2005), using the codes made available in Mildon et al. (2022) (see Electronic Supplement ES6 for input parameters). We parametrize the earthquakes that form each cluster and their recurrence interval during clusters. We assume that earthquake clusters are formed by earthquakes that rupture the fault for its entire length with an earthquake recurrence interval typical of each cluster (clustered recurrence interval). This represents a simplification of the fault slip histories, as we are aware that they could be made of earthquakes with variable magnitudes, slip values and recurrence interval; however, our ^{36}Cl dating modelling does not provide information on single earthquakes, hence we have no information for reproducing variability in these parameters within our modelling. The M and Dmax of these earthquakes are estimated using empirical scaling relationships with the fault length from Wells and Coppersmith (1994). The number of earthquakes forming a cluster is derived by dividing the total amount of slip cumulated during a cluster with the coseismic Dmax obtained from the Dmax/fault length scaling relationship, with non-integer results handled by adding a single earthquake that produces the required surplus slip and ruptures the whole fault length. The clustered recurrence interval is derived by dividing the duration of each cluster with the number of earthquakes forming each cluster (see Electronic Supplement ES6).

These data are used to model earthquakes on the clustered fault and differential stress changes on the receiver fault within the pair. Coulomb stress is converted to differential stress using the equations in King et al. (1994) and Mildon et al. (2022). The geometry of faults at depth is based on their surface traces, with strike-variable fault geometries being made of adjacent rectangular elements of 1 km^2 (e.g. Mildon et al., 2016). We assume that the surface fault geometry continues to depth with the dip measured at the surface. We assume the transition between brittle fault and viscous shear-zone to be at 15 km depth, and we model the shear-zone between 15–24 km maintaining the same geometry of the overlying brittle fault (Cowie et al., 2013). We assume that horizontal strain-rates for the shear-zones match with those of the brittle faults. For each fault/shear-zone, we computed the total differential stress change produced by a complete clustered seismic cycle on the neighbouring fault/shear-zone in the pair, consisting of (i) two coseismic slip events plus (ii) their specific clustered interseismic period characterized by viscous flow (Fig. 3). We did this separately and in turn for both faults within each pair. Coseismic slip events have been modelled so that values of M and Dmax match with those obtained from the Wells and Coppersmith (1994) scaling relationships given measured fault lengths and the assumption of the 15 km depth for the brittle viscous transition

(see Electronic Supplement ES6), except for earthquakes we included to model the non-integer earthquakes defined above, where slip occurred along the entire measured fault length and to 15 km depth, but without honouring the expected slip. This has a minimal effect on our results as we only model the first two earthquakes in a cluster and their intervening interseismic loading to investigate whether calculated stress changes can initiate a cluster on the neighbouring fault. With our approach we can isolate the contribution of along-strike differential stress changes on the occurrence of simultaneous clustering and fault synchronization.

4. Results

We identified six along-strike fault pairs amongst a total of nine fault/shear-zones (Figs. 5 and 6, Table 1). These are characterized by spacing between 1–6 km and average strike changes between 4–45 degrees (Table 1). Specifically: 1) the Mt. Marine and Barisciano-Mt. Stabiata fault/shear-zone pair presents a left-stepping en-echelon arrangement with 1.5 km-spacing and a change in strike of 4 degrees; 2) the Mt. Marine and Paganica-San Demetrio faults/shear-zones have a left-stepping en-echelon arrangement with 4 km-spacing and a change in strike of 11 degrees; 3) the Paganica-San Demetrio and Roccapreturo faults/shear-zones have a right-stepping en-echelon arrangement with 2.3 km-spacing and a change in strike of 17 degrees; 4) the Roccapreturo and Scanno faults/shear-zones have a right-stepping en-echelon arrangement with 6 km-spacing and a change in strike of 25 degrees; 5) the Laga and Campo Imperatore faults/shear-zones have 1 km-spacing, and an abrupt change of strike of 45 degrees; 6) the Fucino and Pescasseroli faults/shear-zones have a right-stepping en-echelon arrangement with 5 km-spacing and a strike change of 10 degrees.

Cosmogenic dating of fault planes reveals that all the nine faults exhibit a clustered behaviour in the Holocene (Fig. 4; Electronic Supplement ES4). The retrieved slip histories generally fall within the last 20 kyrs, except for the Pescasseroli fault, whose preserved slip history begins at ~30 ka. All faults display slip-rates that fluctuate through time, with periods of rapid slip accumulation alternating with periods of slow/no activity. The periods of rapid slip have durations of around 2000–4000 years, and they involve up to 15 m of slip (Table 1). The slip magnitudes exceed the expected coseismic Dmax predicted by the Dmax/fault length scaling relationship of Wells and Coppersmith (1994). We therefore interpret these positive slip-rate fluctuations as earthquake clusters, during which the rapid slip-rate is accommodated by multiple surface-rupturing earthquakes occurring over time scales much shorter than the longer-term average earthquake recurrence interval of the faults.

When comparing the modelled slip histories of faults within the fault/shear-zone pairs, two distinct patterns are observed. Three fault/shear-zone pairs are characterized by the occurrence of simultaneous earthquake clusters: the Mt. Marine and Barisciano fault/shear-zone pair, the Mt. Marine and Paganica-San Demetrio fault/shear-zone pair and the Paganica-San Demetrio and Roccapreturo fault/shear-zone pair (Fig. 5 and Table 1). These three fault/shear-zone pairs have spacing up to 4 km and strike changes not exceeding 17 degrees (Table 1). The other three pairs (the Roccapreturo and Scanno fault/shear-zone pair, the Laga and Campo Imperatore fault/shear-zone pair, the Fucino and Pescasseroli fault/shear-zone pair) show instead non-simultaneous clustering (Fig. 6) and are characterized by larger spacing, up to 6 km, and/or larger strike variation, up to 45 degrees (Fig. 6 and Table 1).

Differential stress modelling associated with every cluster indicates that they all produce positive changes of differential stress on along-strike faults, as expected for along-strike interaction of faults (Figs. 5 and 6). However, there are significant differences in the differential stress changes within pairs that exhibit simultaneous clustering and pairs with non-simultaneous clustering (Fig. 7a and Table 1). We focus our attention at the differential stress changes averaged along the fault at 15–16 km depth, where the viscously deforming material in the shear-zone will have the highest viscosity for each example, limiting the strain passing on to the overlying brittle fault. Firstly, the differential stress changes associated with faults/shear-zones with simultaneous clusters are overall larger than those between faults/shear-zones with non-simultaneous clusters. Secondly, the differential stress changes between faults/shear-zones for each of the two individual calculations for two neighbours with simultaneous clusters tend to be of a more similar magnitude, compared to those on non-simultaneous clusters.

Overall, our results show that fault/shear-zone pairs with lower fault spacing and strike changes are associated with simultaneous earthquake clustering and larger differential stress changes of similar magnitude between the two fault/shear-zones. On the other hand, fault/shear-zone

Table 1
Table summarising the structural arrangement of each fault pair, the attributes of the earthquake clusters studied on every fault and the associated differential stress changes averaged at 15–16 km depth imparted on every receiver fault.

Fault/ Shear-zone pair	Fault spacing (km)	Strike change (degree)	Fault name	Cluster start (±500 yrs)	Cluster end (±500 yrs)	Cluster duration (yrs)	Slip during cluster (m)	Slip-rate during cluster (mm/yr)	Avg. diff. stress at 15–16 km imparted on the receiver fault (MPa)
1	1.5	4	Barisciano-Mt. Stabiata	4050	2000	2050	9	4.4	0.532026
			Mt. Marine	4250	250	4000	15.1	3.77	0.606547
2	4	11	Mt. Marine	4250	250	4000	15.1	3.77	0.634251
			Paganica-San Demetrio	2300	300	2000	5.9	2.95	0.410718
3	2.3	17	Paganica-San Demetrio	2300	300	2000	5.9	2.95	0.292158
			Roccapreturo	2000	0	2000	6.6	3.32	0.394512
4	6	25	Roccapreturo	2000	0	2000	6.6	3.32	0.181593
			Scanno	4600	2200	2400	7.2	3.03	0.542836
5	1	45	Campo Imperatore	5200	2900	2300	11.3	4.9	0.216720
			Laga	12,000	10,000	2000	2.9	2.15	0.193899
6	5	10	Fucino	2500	0	2500	7.2	2.88	0.312346
			Pescasseroli	6900	4500	2400	2.2	0.92	0.186364

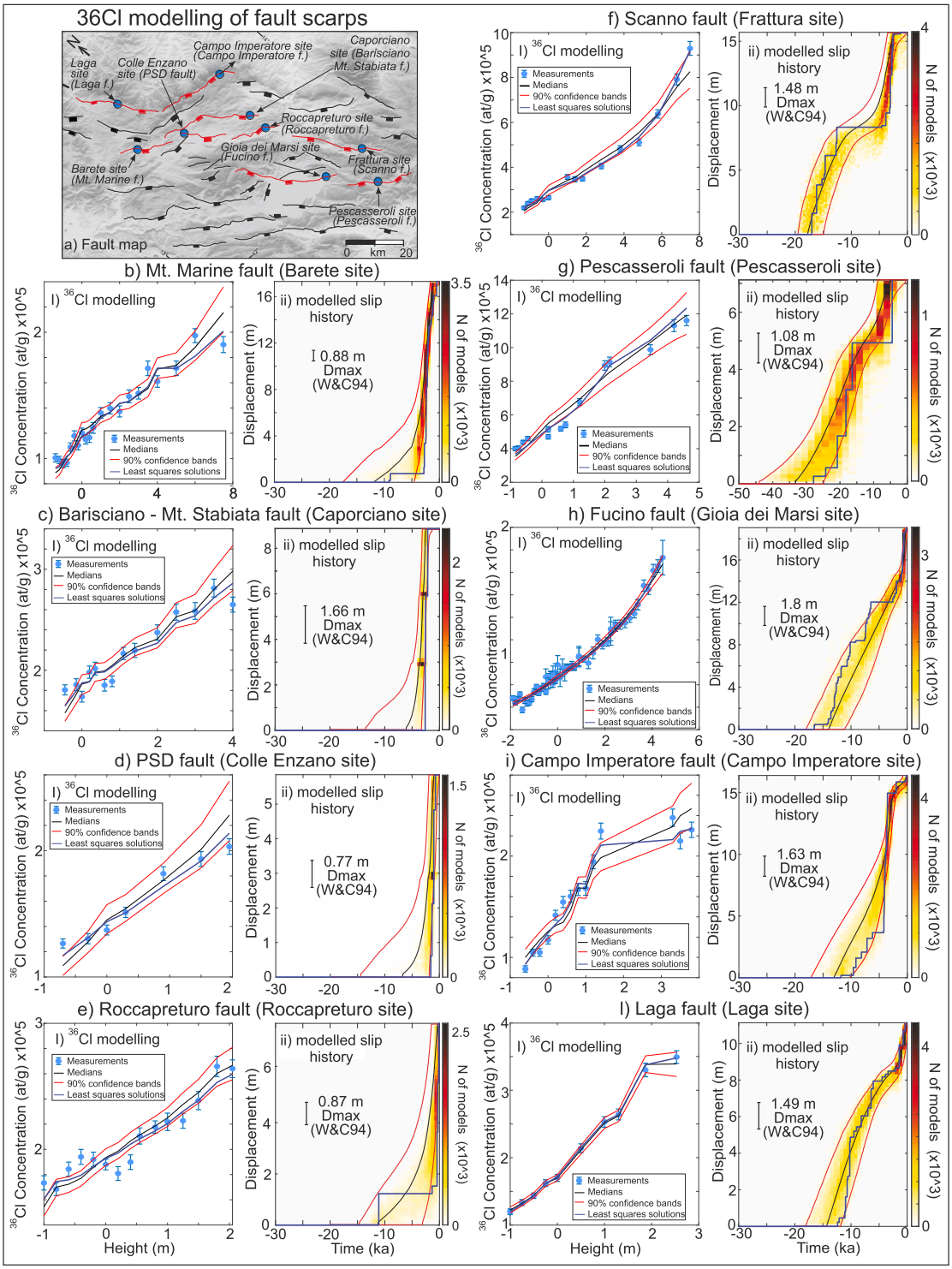

Fig. 4. Cosmogenic ^{36}Cl dating of fault planes. a) Map of the sampling sites. b) Modelling of the ^{36}Cl concentrations and retrieved slip histories. Panels i) show the modelling of ^{36}Cl concentrations up the fault plane. In blue are measurements, blue line is the least squares solutions that represents the best fit of the modelling through the data, red lines are the 90 % confidence bands from the posterior distribution and the black line is the median value, both after 50 % burn-in but calculated over hundreds of thousands of solutions. Panels ii) are the modelled slip histories of the faults retrieved from the ^{36}Cl modelling. In blue is the least squares solution, with density plot of the best 10,000 modelled solutions; red lines are the 90 % confidence bands from the posterior distribution and the black line is the median value, again calculated after 50 % burn-in for hundreds of thousands of solutions. In panels ii) are reported also the maximum displacement (Dmax) values expected for each fault from the Dmax/fault length scaling relationship of Wells and Coppersmith (1994). Site names are referred to the NERC repository within the National Geoscience Data Centre (NGDC) of the British Geological Society and Roberts et al. (2025). Input parameters for each fault are shown in Electronic Supplements S2, detailed output parameters are shown in Electronic Supplements S4.

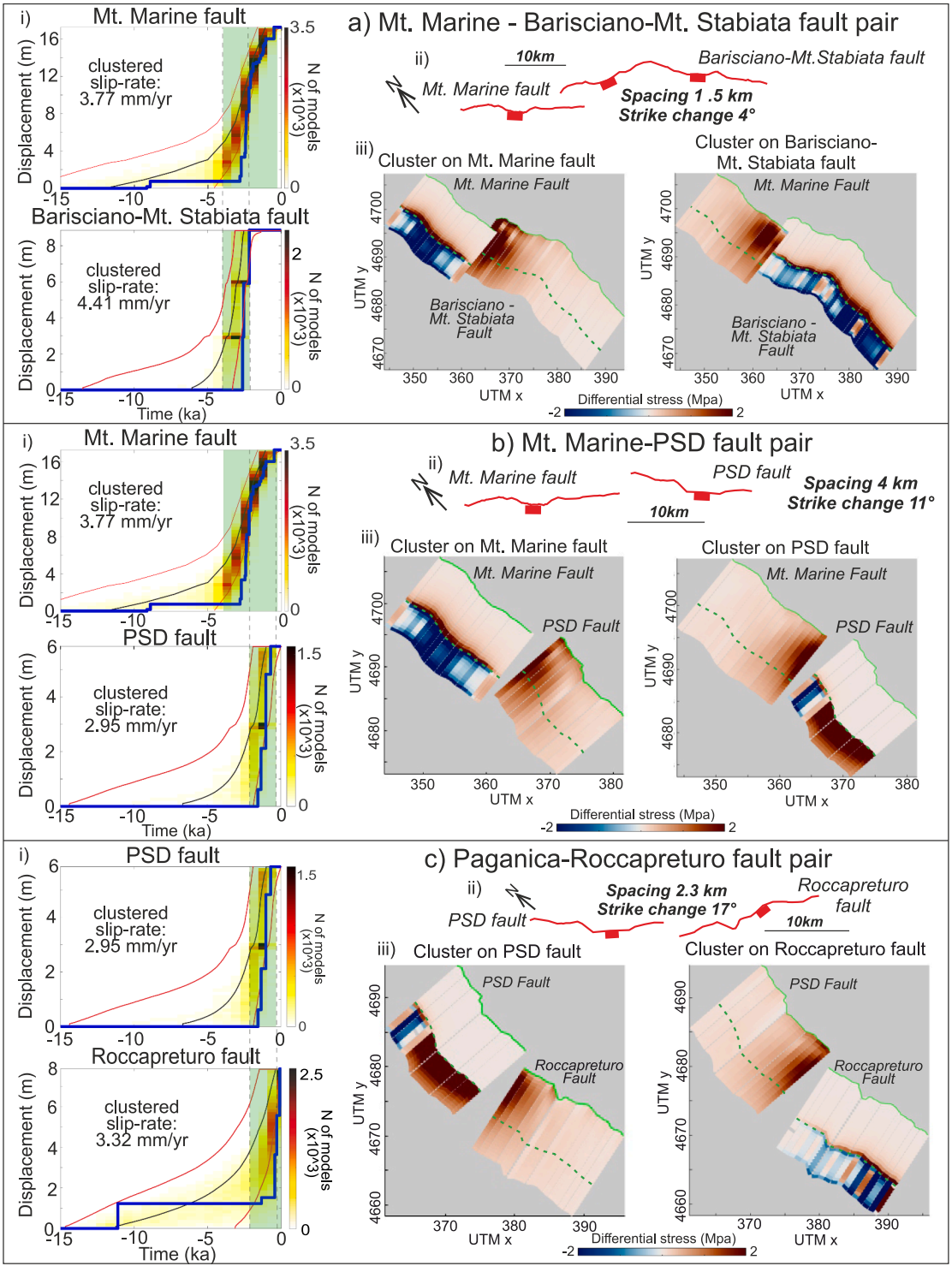

Fig. 5. Analysis of fault/shear-zone pairs with simultaneous clusters. Each panel shows (i) fault maps with values of fault spacing and strike change, (ii) details on the slip histories modelled over the last 15 ka with the studied earthquake clusters highlighted, and (iii) differential stress changes associated with clusters occurring on each fault within the pairs.

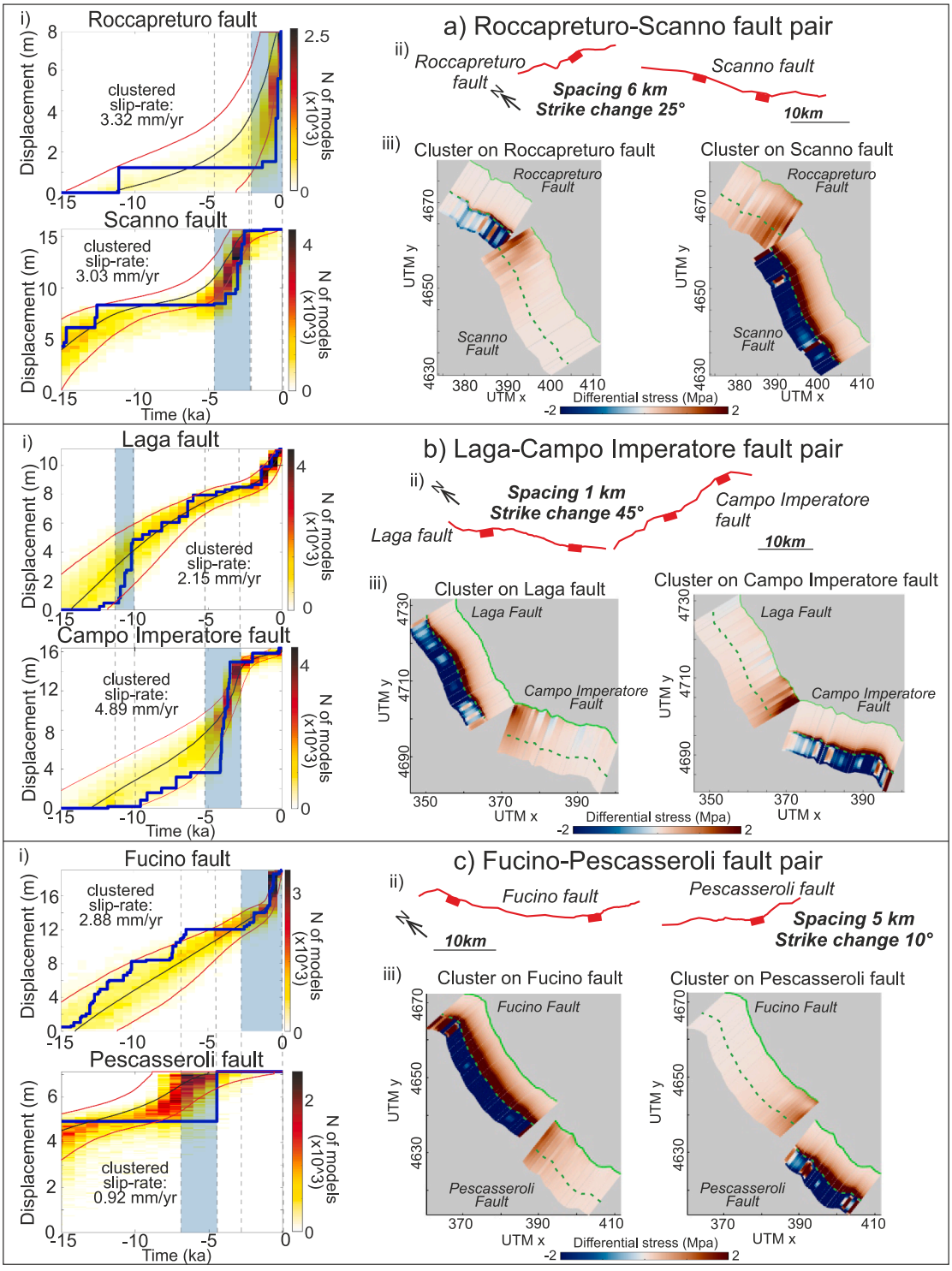

Fig. 6. Analysis of fault/shear-zone pairs with non-simultaneous clusters. Each panel shows (i) fault maps with values of fault spacing and strike change, (ii) details on the slip histories modelled over the last 15 ka with highlighted the studied earthquake clusters, and (iii) differential stress changes associated with clusters occurring on each fault within the pairs.

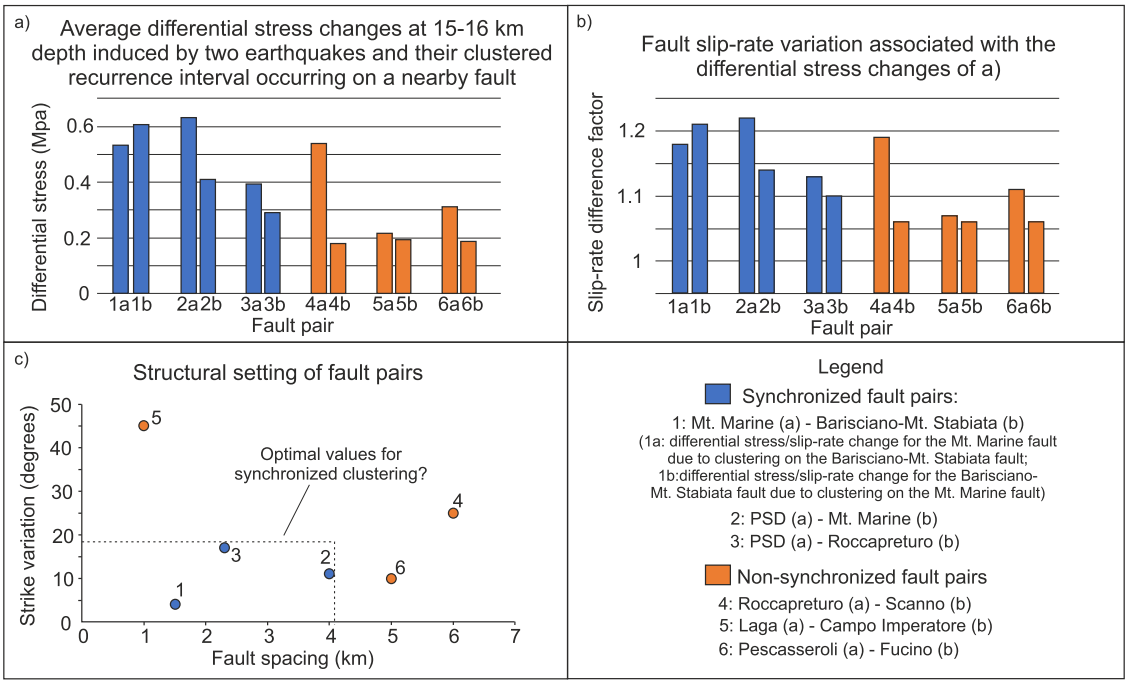

Fig. 7. Discussion of the results. a) Average differential stress changes measured at 15 km depth induced by clustering on the other fault/shear-zone of the pair. It shows that simultaneous clustering coincides with larger and of a similar magnitude differential stress change, compared to pairs with non-simultaneous clustering. b) Slip-rate difference factors due to differential stress variations induced by clustering on the nearby fault within the pair. This plot shows that slip-rate difference factors are larger within synchronized fault pairs than non-synchronized pairs, suggesting that synchronicity of clusters can be prompted by differential stress variations induced by neighbouring clusters. c) Comparisons between strike variations and fault spacing of the multiple fault pairs. It shows that synchronized pairs have lower strike variations and lower fault spacing, suggesting that both characteristics are needed to trigger simultaneous clusters.

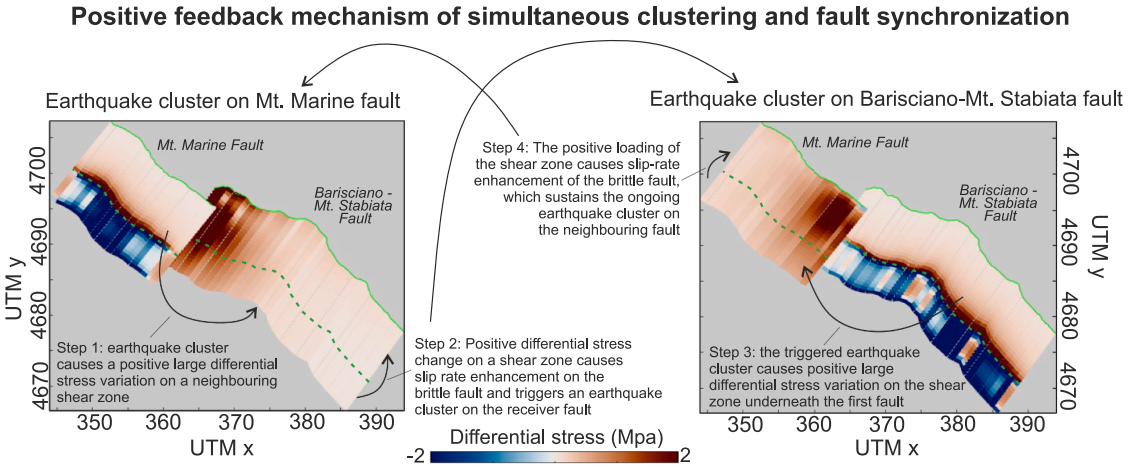

Fig. 8. The positive feedback mechanism of simultaneous clustering and fault synchronization. The occurrence of an earthquake cluster on one fault causes an increase of differential stress on a neighbouring shear-zone (Step 1). This causes slip-rate enhancements on the overlying brittle faults that will enter in an earthquake clustering phase (Step 2). The occurrence of this cluster causes a positive differential stress change on the shear-zone underneath the first fault (Step 3), which will prompt the occurrence of the cluster on the above fault (Step 4). This mechanism shows that synchronization of viscous shear-zones is key for fault synchronization. Negative changes in differential stress shown in plots are associated with the stress reduction due to slip on shear-zones in each calculation; in reality, both shear-zones will be slipping and being positively loaded at the same time.

pairs with larger fault spacing and/or larger strike change show non-simultaneous clustering and either mismatching differential stress changes of lower magnitude and/or stress changes of relatively small magnitude.

5. Discussion

The key result in this study is that the structural setting of along-strike faults acts as a major control on the interaction of neighbouring faults/shear-zones and the occurrence of simultaneous earthquake clustering. The occurrence of coeval earthquake clustering on neighbouring faults is favoured when their structural setting allows for larger and similar differential stress changes between their two neighbouring fault/shear-zones (Fig. 7a). Our results suggest that differential stress changes can induce earthquake clusters also when the largest values of differential stress changes are localised on one portion of the shear-zone. These affect the entire behaviour of the overlying brittle fault, as confirmed by consistency with results provided by ^{36}Cl dating sites

located farther from the largest stress changes modelled on the shear-zones. To verify the relationship between differential stress variations and earthquake clustering, we calculated the slip-rate difference factor of each receiver fault due to differential stress changes on its shear-zone induced by an earthquake cluster on the neighbouring fault (Fig. 7b). To do this, we (1) used Eq. (2) to calculate strain-rates averaged over the entire slip history retrieved with ^{36}Cl dating; (2) we used the same equation to calculate strain-rates following the differential stress changes averaged over 15–16 km depth on the receiver shear-zone (Fig. 7a); (3) we converted the strain-rates into implied slip-rates on the overlying brittle faults, following the notion that finite strain on the brittle fault must equal the finite strain on the viscous shear-zones; (4) we calculated slip-rate difference factors by dividing the slip-rates obtained from strain-rates calculated in (2) with slip-rates derived from strain-rates of point (1) (see Electronic Supplement ES7). Our results show that fault/shear-zone pairs with simultaneous clusters have (i) larger slip-rate enhancement factors, and (ii) similar values of slip-rate enhancement factors within the pair. On the other hand, fault/shear-zone pairs with non-simultaneous clusters show lower slip-rate enhancement factors, or largely different values between the two paired faults/shear-zones. Hence, this is consistent with the hypothesis that a direct link between differential stress changes and the occurrence of simultaneous clustering exists. Larger and similar differential stress changes produce larger and similar slip-rate enhancement factors that we suggest will push both faults/shear-zones into simultaneous clusters, leading therefore towards fault synchronisation (*sensu* Scholz 2010). The consistency between larger slip-rate difference factors and simultaneous clusters on receiver faults represents an independent control that reinforces the idea of fault synchronization due to differential stress changes between favourably oriented neighbouring faults/shear-zones. Our findings follow in principle the mechanism of fault synchronization proposed by Scholz (2010), which was based on mutual positive stress changes over multiple seismic cycles between neighbouring faults. We expand this mechanism by suggesting that synchronization and simultaneous clustered activity of neighbouring faults may be driven by the synchronization of the viscous shear-zones underlying the brittle faults. Repeated earthquakes on one fault produce large differential stress variations on along-strike neighbouring shear-zones that enhance the slip-rate of the overlying fault, which in turn promotes the beginning of an earthquake cluster and induces similar differential stress variations back onto the first shear-zone, causing the enhancement of the slip-rate of its overlying fault (Fig. 8). This process causes the two shear-zones to be positively loaded during the same time window, i.e. the neighbouring shear-zones move towards their synchronization. The simultaneous positive variation of the differential stress on the two shear-zones will coincide with the simultaneous enhancement of the slip-rates of the two overlying brittle faults, which will therefore tend to enter simultaneously in a phase of earthquake clustering, reaching synchronization over timescales of multiple seismic cycles. We suggest that this positive feedback mechanism of synchronization of shear-zones and slip-rate enhancements on overlying brittle faults can be a major driver towards simultaneous earthquake clustering and fault synchronization. Nonetheless, faults with non-simultaneous clustering show positive, although smaller, slip-rate enhancement factors (e.g. fault pairs 4, 5 and 6; Fig. 7b). In these cases, the differential stress changes involved in the along-strike fault interaction appear not to be large enough to have yet driven the seismic cycles of the structures towards synchronization. This suggests that, in order to have fault synchronization, both neighbouring faults/shear-zones need to record relatively large and similar values of differential stress change.

To quantify the characteristics of these favourable settings, we compared values of spacing and strike variation between faults within the studied pairs (Fig. 7c). We refer to values measured at the surface, where we can reasonably define fault geometries, compared to fault geometries at depth, where we mostly lack natural data and they are only reconstructed through modelling. Fault pairs with simultaneous clustering seem to fall within fault spacing $\leq$ 4 km and strike variations of $<$20 degrees, while non-simultaneous fault pairs are more scattered within the plot. These findings support the observation that simultaneous clustering is promoted on faults with low strike change and fault spacing, a setting that allows high stress coupling and the onset of the positive feedback mechanism towards fault synchronization. Discrepancies between the two parameters, for instance small fault spacing but large strike variation, appear not to allow for large stress coupling that will prompt simultaneous clustering on along-strike faults. Similar values of fault spacing and strike variation were already suggested as controls for fault interaction during single earthquakes. For instance, Biasi and Wesnousky (2016; 2017) analysed the propagation of earthquake ruptures over steps and bends, identifying threshold values for simultaneous ruptures of normal faults of 7 km spacing and 50 degrees (although this value refers to generic dip slip faults). Moreover, 5 km fault spacing is commonly considered a spacing threshold for multi-fault earthquakes in fault-based seismic hazard assessments (e.g. Field et al., 2014). Hence, it may be possible that fault interaction over multiple timescales, either that of single earthquakes or that of multiple seismic cycles lasting few millennia, may be driven by the similar geometrical constraints. In other words, the fault arrangement seems to influence fault synchrony at multiple timescales, allowing or not the simultaneous occurrence of single earthquakes and of thousand years-long earthquake clusters. More data are needed to verify the consistency of such structural controls on fault interactions constrained over multiple timescales.

Overall, our work provides new insights into dynamics of active fault and shear-zone systems, with strong implications in seismic hazard assessments. Whilst Mildon et al. (2022) and Roberts et al. (2024; 2025) suggests that reduction in differential stress on brittle faults/viscous shear zones due to across-strike interaction may lead a fault into an anticluster period, this paper shows that along-strike interaction may lead a fault into a clustered period. All together, these findings suggest that it is possible to identify patterns of faults that are more likely to enter in either earthquake clusters or anticlusters based on their structural arrangement relative to one another. This highlights the importance of identifying the arrangement and geometry of faults in a network as this represents a major control on driving stress transfer that converts into likelihood patterns of seismic hazard within a network of active faults. We recommend more studies implying long-term slip-rate fluctuations and variable structural arrangements in order to improve our knowledge on the threshold values in fault spacing, either along- and across-strike, and strike changes that allow for synchronized and out-of-synchrony fault/shear-zone behaviours.

6. Conclusions

The combination of cosmogenic ^{36}Cl dating and differential stress modelling provides key insight to investigate the processes associated with fault interaction over multiple seismic cycles. We can envisage a process for the occurrence of simultaneous earthquake clustering and fault synchronization based on the fault spacing and strike changes between along-strike normal faults. Specific along-strike settings, with low fault spacing and low strike change between the adjacent faults, allows for larger differential stress variations between the fault/shear-zones during earthquakes; this converts into larger positive slip-rate different factors that will lead both faults into a phase of earthquake clustering, driving the faults towards synchronization. If faults are not favourably oriented, differential stress variations are lower or non-even between the faults, and this will coincide with positive slip-rate difference factors that are not large enough to alter the seismic cycle of faults. This mechanism suggests that, to have fault synchronization and simultaneous clustering, viscous shear-zones underneath the brittle faults must be synchronized. This process has implications in understanding the dynamics of active faults, the interaction processes of interconnected fault systems and in seismic hazard assessments.

CRediT authorship contribution statement

F. Iezzi: Conceptualization, Formal analysis, Investigation, Methodology, Writing – original draft. **C. Sgambato:** Investigation, Validation, Writing – review & editing. **G. Roberts:** Conceptualization, Data curation, Funding acquisition, Project administration, Writing – review & editing, Supervision. **Z. Mildon:** Methodology, Validation, Writing – review & editing. **J. Robertson:** Validation, Writing – review & editing. **J. Faure Walker:** Funding acquisition, Validation, Writing – review & editing. **I. Papanikolaou:** Validation, Writing – review & editing. **A.M. Michetti:** Validation, Writing – review & editing. **S. Mitchell:** Validation, Writing – review & editing. **R. Shanks:** Data curation, Writing – review & editing. **R. Phillips:** Data curation, Writing – review & editing. **K.J.W. McCaffrey:** Conceptualization, Funding acquisition, Validation, Writing – review & editing. **E. Vittori:** Validation, Writing – review & editing.

Declaration of competing interest

The authors declare that they have no known competing financial interests or personal relationships that could have appeared to influence the work reported in this paper.

Acknowledgements

The study was funded by NERC Grants NE/E01545X/1, NE/I024127/1, NE/ J016497/1 and NE/V012894/1. Patience Cowie contributed to the development of the approaches adopted in this paper. We thank John McCloskey for discussions. Laura Gregory is acknowledged for contributing to fieldwork, field sampling, conducting some of the ^{36}Cl chemistry prior to AMS and initial discussions. Luke Wedmore is acknowledged for contributing to fieldwork, LiDAR studies and initial discussions. We thank the Editor Jean-Philippe Avouac and two anonymous reviewers for comments that helped improving the manuscript. Open access funding provided by Università degli Studi di Napoli Federico II within the CRUI-CARE Agreement.

Supplementary materials

Supplementary material associated with this article can be found, in the online version, at doi:10.1016/j.epsl.2025.119686.

Data availability

Data will be made available on request.

References

Allison, K.L., Dunham, E.M., 2018. Earthquake cycle simulations with rate-and-state friction and power-law viscoelasticity. Tectonophysics. 733, 232–256. https://doi.org/10.1016/j.tecto.2017.10.021.

Anderson, H., Jackson, J., 1987. Active tectonics of the Adriatic region. Geophys. J. Int. 91 (3), 937–983. https://doi.org/10.1111/j.1365-246X.1987.tb01675.

Beck, J., Wolfers, S., Roberts, G.P., 2018. Bayesian earthquake dating and seismic hazard assessment using chlorine-36 measurements (BED v1). Geosci. Model Dev. (GMD) 11 (11), 4383–4397. https://doi.org/10.5194/gmd-11-4383-2018.

Benedetti, L., Manighetti, I., Gaudemer, Y., Finkel, R., Malavieille, J., Pou, K., Arnold, M., Aumaître, G., Bourl`es, D., Keddadouche, K., 2013. Earthquake synchrony and clustering on Fucino faults (Central Italy) as revealed from in situ 36Cl exposure dating. J. Geophys. Res. Solid. Earth. 118 (9), 4948–4974. https://doi.org/10.1002/jgrb.50299.

Biasi, G.P., Wesnousky, S.G., 2016. Steps and gaps in ground ruptures: empirical bounds on rupture propagation. Bull. Seismol. Soc. Am. 106, 1110–1124. https://doi.org/10.1785/0120150175.

Biasi, G.P., Wesnousky, S.G., 2017. Bends and ends of surface ruptures. Bull. Seismol. Soc. Am. 107 (6), 2543–2560. https://doi.org/10.1785/0120160292.

Blumetti, A.M., Di Manna, P., Comerci, V., Guerrieri, L., Vittori, E., 2017. Paleoseismicity of the san demetrio ne' Vestini fault (L'Aquila basin, Central Italy): implications for seismic hazard. Quaternary international 451, 129–142. https://doi.org/10.1016/j.quaint.2016.12.039.

Boncio, P., Lavecchia, G., Pace, B., 2004. Defining a model of 3D seismogenic sources for seismic Hazard Assessment applications: the case of central Apennines (Italy). J. Seismol. 8 (3), 407–425. https://doi.org/10.1023/B:JOSE.0000038449.78801.05.

Boncio, P., Pizzi, A., Brozzetti, F., Pomposo, G., Lavecchia, G., Di Naccio, D., Ferrarini, F., 2010. Coseismic ground deformation of the 6 April 2009 L'Aquila earthquake (central Italy, Mw6. 3). Geophys. Res. Lett. 37 (6). https://doi.org/10.1029/2010GL042807.

Bosi, C., 1975. Osservazioni preliminari su faglie probabilmente attive nell'Appennino centrale. Boll. Soc. Geol. Ital. 94 (4), 827–859.

Cavinato, G.P., De Celles, P.G., 1999. Extensional basins in the tectonically bimodal central Apennines fold-thrust belt, Italy: response to corner flow above a subducting slab in retrograde motion. Geology. 27 (10), 955–958. https://doi.org/10.1130/0091-7613(1999)027<0955:EBITTB>2.3.CO;2.

Cinti, F.R., Pantosti, D., Lombardi, A.M., Civico, R., 2021. Modeling of earthquake chronology from paleoseismic data: insights for regional earthquake recurrence and earthquake storms in the Central Apennines. Tectonophysics. 816, 229016. https://doi.org/10.1016/j.tecto.2021.229016.

Cowie, P.A., Roberts, G.P., Bull, J.M., Visini, F., 2012. Relationships between fault geometry, slip rate variability and earthquake recurrence in extensional settings. Geophys. J. Int. 189 (1), 143–160. https://doi.org/10.1111/j.1365-246X.2012.05378.x.

Cowie, P.A., Scholz, C.H., Roberts, G.P., Faure Walker, J.P., Steer, P., 2013. Viscous roots of active seismogenic faults revealed by geologic slip rate variations. Nat. Geosci. 6 (12), 1036–1040. https://doi.org/10.1038/ngeo1991.

Cowie, P.A., Phillips, R.J., Roberts, G.P., McCaffrey, K., Zijerveld, L.J.J., Gregory, L.C., Faure Walker, J., Wedmore, L.N.J., Dunai, T.J., Binnie, S.A., Freeman, S.P.H.T., 2017. Orogen-scale uplift in the central Italian Apennines drives episodic behaviour of earthquake faults. Sci. Rep. 7 (1), 44858. https://doi.org/10.1038/srep44858.

D'Agostino, N., Mantenuto, S., D'Anastasio, E., Giuliani, R., Mattone, M., Calcaterra, S., Gambino, P., Bonci, L., 2011. Evidence for localized active extension in the central Apennines (Italy) from global positioning system observations. Geology. 39 (4), 291–294. https://doi.org/10.1130/G31796.1.

Daout, S., d'Agostino, N., Pathier, E., Socquet, A., Lavé, J., Doin, M.P., Reisner, M., Benedetti, L., 2023. Along-strike variations of strain partitioning within the Apennines determined from large-scale multi-temporal InSAR analysis. Tectonophysics. 867, 230076. https://doi.org/10.1016/j.tecto.2023.230076.

Dawood, R., Matmon, A., Benedetti, L., ASTER Team, Siman-Tov, S., 2024. Multi-segment earthquake clustering as inferred from 36Cl exposure dating, the Bet Kerem fault system, northern Israel. Tectonics. 43 (5), e2023TC007953. https://doi.org/10.1029/2023TC007953.

Devoti, R., d'Agostino, N., Serpelloni, E., Pietrantonio, G., Riguzzi, F., Avallone, A., Cavaliere, A., Cheloni, D., Cecere, G., D'Ambrosio, C., Falco, L., Selvaggi, G., Metois, M., Esposito, A., Sepe, V., Galvani, A., Anzidei, M., 2017. A combined velocity field of the Mediterranean region. Annals of Geophysics. https://doi.org/10.4401/ag-7059.

Dolan, J.F., Bowman, D.D., Sammis, C.G., 2007. Long-range and long-term fault interactions in Southern California. Geology. 35 (9), 855–858. https://doi.org/10.1130/G23789A.1.

Dolan, J.F., Meade, B.J., 2017. A comparison of geodetic and geologic rates prior to large strike-slip earthquakes: a diversity of earthquake-cycle behaviors? G-cubed 18 (12), 4426–4436. https://doi.org/10.1002/2017GC007014.

Ellis, S., Stockhert, B., 2004. Elevated stresses and creep rates beneath the brittle-ductile transition caused by seismic faulting in the upper crust. J. Geophys. Res. Solid. Earth. 109 (B5). https://doi.org/10.1029/2003JB002744.

Falcucci, E., Gori, S., Moro, M., Fubelli, G., Saroli, M., Chiarabba, C., Galadini, F., 2015. Deep reaching versus vertically restricted quaternary normal faults: implications on seismic potential assessment in tectonically active regions: lessons from the middle Aterno valley fault system, central Italy. Tectonophysics. 651, 186–198.

Faure Walker, J.P., Roberts, G.P., Sammonds, P.R., Cowie, P., 2010. Comparison of earthquake strains over 10^2 and 10^4 year timescales: insights into variability in the seismic cycle in the central Apennines, Italy. J. Geophys. Res. Solid. Earth. 115 (B10). https://doi.org/10.1029/2009JB006462.

Faure Walker, J.P., Roberts, G.P., Cowie, P.A., Papanikolaou, I., Michetti, A.M., Sammonds, P., Wilkinson, M., McCaffrey, K.J.W., Phillips, R.J., 2012. Relationship between topography, rates of extension and mantle dynamics in the actively-extending Italian Apennines. Earth. Planet. Sci. Lett. 325, 76–84. https://doi.org/10.1016/j.epsl.2012.01.028.

Faure Walker, J.P., Visini, F., Roberts, G., Galasso, C., McCaffrey, K., Mildon, Z., 2019. Variable fault geometry suggests detailed fault-slip-rate profiles and geometries are needed for fault-based probabilistic seismic hazard assessment (PSHA). Bulletin of the Seismological Society of America 109 (1), 110–123. https://doi.org/10.1785/0120180137.

Faure Walker, J., Boncio, P., Pace, B., Roberts, G., Benedetti, L., Scotti, O., Visini, F., Peruzza, L., 2021. Fault2SHA Central Apennines database and structuring active fault data for seismic hazard assessment. Sci. Data 8 (1), 87. https://doi.org/10.1038/s41597-021-00868-0.

Field, E.H., Arrowsmith, R.J., Biasi, G.P., Bird, P., Dawson, T.E., Felzer, K.R., Jackson, D. D., Johnson, K.M., Jordan, T.H., Madden, C., Michael, A.J., Milner, K.R., Page, M.T., Parsons, T., Powers, P.M., Shaw, B.E., Thatcher, W.R., Weldon, R.J., Zeng, Y., 2014. Uniform California earthquake rupture forecast, version 3 (UCERF3) — The time-independent model. Bull. Seismol. Soc. Am. 104 (3), 1122–1180. https://doi.org/10.1785/0120130164.

Fossen, H., Cavalcante, G.C.G., 2017. Shear zones—A review. Earth-Sci. Rev. 171, 434–455. https://doi.org/10.1016/j.earscirev.2017.05.002.

Galadini, F., Galli, P., 1999. The Holocene paleoearthquakes on the 1915 Avezzano earthquake faults (central Italy): implications for active tectonics in the central

Apennines. Tectonophysics. 308 (1–2), 143–170. https://doi.org/10.1016/S0040-1951(99)00091-8.
Galadini, F., Galli, P., 2003. Paleoseismology of silent faults in the Central Apennines (Italy): the Mt. Vettore and Laga Mts. Faults. Annals of Geophysics. https://doi.org/10.4401/ag-3457.
Galli, P., Galadini, F., Pantosti, D., 2008. Twenty years of paleoseismology in Italy. Earth. Sci. Rev. 88 (1–2), 89–117. https://doi.org/10.1016/j.earscirev.2008.01.001.
Galli, P.A., Giaccio, B., Messina, P., Peronace, E., Zuppi, G.M., 2011. Palaeoseismology of the L'Aquila faults (central Italy, 2009, M w 6.3 earthquake): implications for active fault linkage. Geophysical Journal International, 187 (3), 1119–1134. https://doi.org/10.1111/j.1365-246X.2011.05233.x.
Galli, P., Galderisi, A., Messina, P., Peronace, E., 2022. The Gran Sasso fault system: paleoseismological constraints on the catastrophic 1349 earthquake in Central Italy. Tectonophysics. 822, 229156. https://doi.org/10.1016/j.tecto.2021.229156.
Goodall, H.J., Gregory, L.C., Wedmore, L.N., McCaffrey, K.J.W., Amey, R.M.J., Roberts, G.P., Shanks, R.P., Phillips, R.J., Hooper, A., 2021. Determining histories of slip on normal faults with bedrock scarps using cosmogenic nuclide exposure data. Tectonics. 40 (3), e2020TC006457. https://doi.org/10.1029/2020TC006457.
Goldfinger, C., Ikeda, Y., Yeats, R.S., Ren, J., 2013. Superquakes and supercycles. Seismological Res. Lett. 84 (1), 24–32. https://doi.org/10.1785/0220110135.
Hirth, G., Teyssier, C., Dunlap, J.W., 2001. An evaluation of quartzite flow laws based on comparisons between experimentally and naturally deformed rocks. Int. J. Earth. Sci. 90, 77–87. https://doi.org/10.1007/s005310000152.
Iezzi, F., Roberts, G., Faure Walker, J., Papanikolaou, I., Ganas, A., Deligiannakis, G., Beck, J., Wolfers, S., Gheorghiu, D., 2021. Temporal and spatial earthquake clustering revealed through comparison of millennial strain-rates from 36Cl cosmogenic exposure dating and decadal GPS strain-rate. Sci. Rep. 11 (1), 23320. https://doi.org/10.1038/s41598-021-02131-3.
Iezzi, F., Francescone, M., Pizzi, A., Blumetti, A., Boncio, P., Di Manna, P., Pace, B., Piacentini, T., Papasodaro, F., Morelli, F., Caciagli, M., Chiappini, M., D'Ajello Caracciolo, F., Materni, V., Nicolosi, I., Sapia, V., Urbini, S., 2023. Slip localization on multiple fault splays accommodating distributed deformation across normal fault complexities. Tectonophysics. 868, 230075. https://doi.org/10.1016/j.tecto.2023.230075.
King, G.C., Stein, R.S., Lin, J., 1994. Static stress changes and the triggering of earthquakes. Bull. Seismol. Soc. Am. 84 (3), 935–953.
Mildon, Z.K., Toda, S., Faure Walker, J.P., Roberts, G.P., 2016. Evaluating models of Coulomb stress transfer: is variable fault geometry important? Geophys. Res. Lett. 43 (24), 12407–12414.
Mildon, Z.K., Roberts, G.P., Faure Walker, J.P., Iezzi, F., 2017. Coulomb stress transfer and fault interaction over millennia on non-planar active normal faults: the M w 6.5–5.0 seismic sequence of 2016–2017, central Italy. Geophys. J. Int. 210 (2), 1206–1218. https://doi.org/10.1093/gji/ggx213.
Mildon, Z.K., Roberts, G.P., Faure Walker, J.P., Toda, S., 2019. Coulomb pre-stress and fault bends are ignored yet vital factors for earthquake triggering and hazard. Nat. Commun. 10 (1), 2744. https://doi.org/10.1038/s41467-019-10520-6.
Mildon, Z.K., Roberts, G.P., Faure Walker, J.P., Beck, J., Papanikolaou, I., Michetti, A.M., Toda, S., Iezzi, F., Campbell, L., McCaffrey, K.J., Shanks, R., 2022. Surface faulting earthquake clustering controlled by fault and shear-zone interactions. Nat. Commun. 13 (1), 7126. https://doi.org/10.1038/s41467-022-34821-5.
Mechernich, S., Schneiderwind, S., Mason, J., Papanikolaou, I.D., Deligiannakis, G., Pallikarakis, A., Binnie, S.A., Dunai, T.J., Reicherter, K., 2018. The seismic history of the Pisia fault (eastern Corinth rift, Greece) from fault plane weathering features and cosmogenic 36Cl dating. J. Geophys. Res. Solid. Earth. 123, 4266–4284. https://doi.org/10.1029/2017JB014600.
Mechernich, S., Reicherter, K., Deligiannakis, G., Papanikolaou, I., 2023. Tectonic geomorphology of active faults in Eastern Crete (Greece) with slip rates and earthquake history from cosmogenic 36Cl dating of the Lastros and Orno faults. Quater. Int. 651, 77–91. https://doi.org/10.1016/j.quaint.2022.04.007.
Mozafari, N., Tikhomirov, D., Sumer, Ö., Özkaymak, Ç., Uzel, B., Yeşilyurt, S., Ivy-Ochs, S., Vockenhuber, C., Sözbilir, H., Akçar, N., 2019. Dating of active normal fault scarps in the Büyük Menderes Graben (western Anatolia) and its implications for seismic history. Quat. Sci. Rev. 220, 111–123. https://doi.org/10.1016/j.quascirev.2019.07.002.
Oskin, M., Perg, L., Shelef, E., Strane, L., Gurney, E., Singer, B., Zhang, X., 2008. Elevated shear zone loading rate during an earthquake cluster in eastern California. Geology. 36 (6), 507–510. https://doi.org/10.1130/G24814A.1.
Pace, B., Bocchini, G.M., Boncio, P., 2014. Do static stress changes of a moderate magnitude earthquake significantly modify the regional seismic hazard? Hints from the L'Aquila 2009 normal-faulting earthquake (Mw 6.3, central Italy). Terra Nova 26 (6), 430–439. https://doi.org/10.1111/ter.12117.
Palumbo, L., Benedetti, L., Bourles, D., Cinque, A., Finkel, R., 2004. Slip history of the Magnola fault (Apennines, Central Italy) from 36Cl surface exposure dating: evidence for strong earthquakes over the holocene. Earth. Planet. Sci. Lett. 225 (1–2), 163–176. https://doi.org/10.1016/j.epsl.2004.06.012.
Pantosti, D., D'Addezio, G., Cinti, F.R., 1996. Paleoseismicity of the Ovindoli-Pezza fault, central Apennines, Italy: a history including a large, previously unrecorded earthquake in the Middle ages (860–1300 AD). J. Geophys. Res.: Solid Earth 101 (B3), 5937–5959. https://doi.org/10.1029/95JB03213.
Papanikolaou, I.D., Roberts, G.P., Michetti, A.M., 2005. Fault scarps and deformation rates in Lazio–Abruzzo, Central Italy: comparison between geological fault slip-rate and GPS data. Tectonophysics. 408 (1–4), 147–176. https://doi.org/10.1016/j.tecto.2005.05.043.
Piccardi, L., Gaudemer, Y., Tapponnier, P., Boccaletti, M., 1999. Active oblique extension in the central Apennines (Italy): evidence from the Fucino region. Geophys. J. Int. 139 (2), 499–530. https://doi.org/10.1046/j.1365-246X.1999.00955.x.
Pizzi, A., Galadini, F., 2009. Pre-existing cross-structures and active fault segmentation in the northern-central Apennines (Italy). Tectonophysics. 476 (1–2), 304–319. https://doi.org/10.1016/j.tecto.2009.03.018.
Roberts, G.P., Michetti, A.M., 2004. Spatial and temporal variations in growth rates along active normal fault systems: an example from the Lazio–Abruzzo Apennines, central Italy. J. Struct. Geol. 26 (2), 339–376. https://doi.org/10.1016/S0191-8141(03)00103-2.
Roberts, G.P., Sgambato, C., Mildon, Z.K., Iezzi, F., Beck, J., Robertson, J., Papanikolaou, I., Michetti, A.M., Faure Walker, J.P., Meschis, M., Shanks, R., Phillips, R., McCaffrey, K.J.W., Vittori, E., Mitchell, S., 2024. Spatial migration of temporal earthquake clusters driven by the transfer of differential stress between neighbouring fault/shear-zone structures. J. Struct. Geol. 181, 105096. https://doi.org/10.1016/j.jsg.2024.105096.
Roberts, G., Iezzi, F., Sgambato, C., Robertson, J., Beck, J., Mildon, Z.K., Papanikolaou, I., Michetti, A.M., Faure Walker, J.P., Mitchell, S., Meschis, M., Shanks, R., Phillips, R., McCaffrey, K.J.W., Vittori, E., Visini, F., Iqbal, M., 2025. Characteristics and modelling of slip-rate variability and temporal earthquake clustering across a distributed network of active normal faults constrained by in situ ^{36}Cl cosmogenic dating of fault scarp exhumation, central Italy. J. Struct. Geol. 195, 105391. https://doi.org/10.1016/j.jsg.2025.105391.
Rovida, A., Locati, M., Camassi, R., Lolli, B., Gasperini, P., Antonucci, A., 2022. Catalogo Parametrico dei Terremoti Italiani (CPTI15), Versione 4.0 [Data Set]. Istituto Nazionale di Geofisica e Vulcanologia (INGV). https://doi.org/10.13127/cpti/cpti15.4.
Rovida, A., Locati, M., Camassi, R., Lolli, B., Gasperini, P., 2020. The Italian earthquake catalogue CPTI15. Bull. Earthq. Eng. 18 (7), 2953–2984. https://doi.org/10.1007/s10518-020-00818-y.
Salditch, L., Stein, S., Neely, J., Spencer, B.D., Brooks, E.M., Agnon, A., Liu, M., 2020. Earthquake supercycles and long-term fault memory. Tectonophysics. 774, 228289. https://doi.org/10.1016/j.tecto.2019.228289.
Shimamoto, T., Noda, H., 2014. A friction to flow constitutive law and its application to a 2-D modeling of earthquakes. J. Geophys. Res. Solid. Earth. 119 (11), 8089–8106. https://doi.org/10.1002/2014JB011170.
Schlagenhauf, A., Gaudemer, Y., Benedetti, L., Manighetti, I., Palumbo, L., Schimmelpfennig, I., Finkel, R., Pou, K., 2010. Using in situ chlorine-36 cosmonuclide to recover past earthquake histories on limestone normal fault scarps: a reappraisal of methodology and interpretations. Geophys. J. Int. 182 (1), 36–72. https://doi.org/10.1111/j.1365-246X.2010.04622.x.
Scholz, C.H., 2010. Large earthquake triggering, clustering, and the synchronization of faults. Bulletin Seismol. Society Am. 100 (3), 901–909. https://doi.org/10.1785/0120090309.
Sieh, K., Natawidjaja, D.H., Meltzner, A.J., Shen, C.C., Cheng, H., Li, K.S., Suwargadi, B. W., Galetzka, J., Philibosian, B., Edwards, R.L., 2008. Earthquake supercycles inferred from sea-level changes recorded in the corals of west Sumatra. Science (1979) 322 (5908), 1674–1678. http://doi.org/10.1126/science.1163589.
Stone, J., Allan, G., Fifield, L., Cresswell, R., 1996. Cosmogenic chlorine-36 from calcium spallation. Geochim. Cosmochim. Acta. 60, 679–692.
Tesson, J., Benedetti, L., 2019. Seismic history from in situ 36Cl cosmogenic nuclide data on limestone fault scarps using Bayesian reversible jump Markov chain Monte Carlo. Quat. Geochronol. 52, 1–20. https://doi.org/10.1016/j.quageo.2019.02.004.
Tesson, J., Pace, B., Benedetti, L., Visini, F., Delli Rocioli, M., Arnold, M., Aumaître, G., Bourlès, D.L., Keddadouche, K., 2016. Seismic slip history of the Pizzalto fault (central Apennines, Italy) using in situ-produced 36Cl cosmic ray exposure dating and rare earth element concentrations. J. Geograph. Res.: Solid Earth 121 (3), 1983–2003.
Tikhomirov, D., Mozafari, N., Ivy-Ochs, S., Alfimov, V., Vockenhuber, Ch., Akçar, N., 2019. Fault Scarp Dating Tool - a MATLAB code for fault scarp dating with in-situ chlorine-36 along with datasets of Yavansu and Kalafat faults. Data Brief. 26, 104476. https://doi.org/10.1016/j.dib.2019.104476.
Toda, S., Stein, R.S., Richards-Dinger, K., Bozkurt, S.B., 2005. Forecasting the evolution of seismicity in southern California: animations built on earthquake stress transfer. J. Geophys. Res. 110, B05S16. https://doi.org/10.1029/2004JB003415.
Verdecchia, A., Pace, B., Visini, F., Scotti, O., Peruzza, L., Benedetti, L., 2018. The role of viscoelastic stress transfer in long-term earthquake cascades: insights after the central Italy 2016–2017 seismic sequence. Tectonics. 37 (10), 3411–3428.
Visini, F., Pace, B., 2014. Insights on a key parameter of earthquake forecasting, the coefficient of variation of the recurrence time, using a simple earthquake simulator. Seismol Res. Lett. 85, 703–713. https://doi.org/10.1785/0220130165.
Wells, D.L., Coppersmith, K.J., 1994. New empirical relationships among magnitude, rupture length, rupture width, rupture area, and surface displacement. Bull. Seismol. Soc. Am. 84 (4), 974–1002. https://doi.org/10.1785/BSSA0840040974.